

Bent Keto Form of Curcumin, Preferential Stabilization of Enol by Piperine, and Isomers of Curcumin \cap Cyclodextrin Complexes: Insights from Ion Mobility Mass Spectrometry

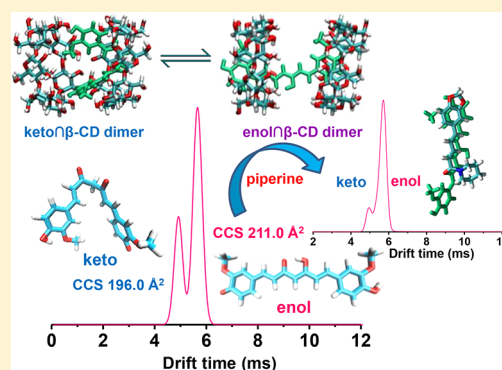
Abhijit Nag,[†] Papri Chakraborty,[†] Ganapati Natarajan,[†] Ananya Bakshi,[†] Sathish Kumar Mudedla,[‡] Venkatesan Subramanian,[‡] and Thalappil Pradeep^{*,†}

[†]DST Unit of Nanoscience and Thematic Unit of Excellence, Department of Chemistry, Indian Institute of Technology Madras, Chennai-600036, India

[‡]Chemical Laboratory, CSIR-Central Leather Research Institute, Adyar, Chennai 600020, India

Supporting Information

ABSTRACT: A detailed examination of collision cross sections (CCSs) coupled with computational methods has revealed new insights into some of the key questions centered around curcumin, one of the most intensively studied natural therapeutic agents. In this study, we have distinguished the structures and conformers of the well-known enol and the far more elusive keto form of curcumin by using ion mobility mass spectrometry (IM MS). The values of the theoretically predicted isomers were compared with the experimental CCS values to confirm their structures. We have identified a bent structure for the keto form and the degree of bending was estimated. Using IM MS, we have also shown that ESI MS reflects the solution phase structures and their relative populations, in this case. Piperine, a naturally occurring heterocyclic compound, is known to increase the bioavailability of curcumin. However, it is still not clearly understood which tautomeric form of curcumin is better stabilized by it. We have identified preferential stabilization of the enol form in the presence of piperine using IM MS. Cyclodextrins (CDs) are used as well-known carriers in the pharmaceutical industry for increasing the stability, solubility, bioavailability, and tolerability of curcumin. However, the crystal structures of supramolecular complexes of curcumin \cap CD are unknown. We have determined the structures of different isomers of curcumin \cap CD (α - and β -CD) complexes by comparing the CCSs of theoretically predicted structures with the experimentally obtained CCSs, which will further help in understanding the specific role of the structures involved in different biological activities.



Many of the chemical and pharmacological details of curcumin, one of the most intensely investigated biomolecules with long history, are still unknown. The molecule even now is the subject of over 1400 publications annually.¹ It is known that two tautomeric forms of curcumin, namely, keto and enol, exist in solution,² and they have been detected by various tools such as nuclear magnetic resonance spectroscopy (NMR).² The crystal structure of the enol form and its planar conformation can be deduced from X-ray diffraction,³ while the conformation of the keto form is known with much less certainty due to the lack of single crystal data, excepting that of a cocrystal with 4,4'-bipyridine-*N,N'*-dioxide, which shows a planar keto structure.⁴ This might be due to inherent structural asymmetries in the keto isomer arising from conformational freedom around the keto $-C-(CO)-C-(CO)-C-$ bonds, which inhibits crystallization. The solution phase structure of curcumin is also of great importance due to its biological^{5–8} and pharmacological activities including antitumor,⁹ antioxidant,^{10,11} anti-inflammatory,^{12,13} anti-HIV¹⁴ (human immunodeficiency virus), anti-Alzheimer's,^{15–17} anticancer,^{18,19} antihepatotoxic,²⁰ and cardio-

vascular protection activities.²¹ The keto form is important in certain biochemical reactions and biological activities. The "NADPH-dependent curcumin/dihydrocurcumin reductase" enzyme acts on the keto form of curcumin to form tetrahydrocurcumin,²² whereas the enol is the active form for the control of Alzheimer's disease.²³ Furthermore, it is also very difficult to detect the conformation of the keto form from NMR data in the solution phase. Simple isolation of these species and their quantitation will be useful from many perspectives as both these forms are different in biological activity.

The possible conformational keto isomers have so far been predicted only theoretically,^{24,25} by comparative energy analysis of different conformers obtained using various approaches such as force-field conformer searches, molecular dynamics and density functional theory (DFT). However, these predicted keto structures²⁴ have not been verified

Received: December 15, 2017

Accepted: July 11, 2018

Published: July 11, 2018

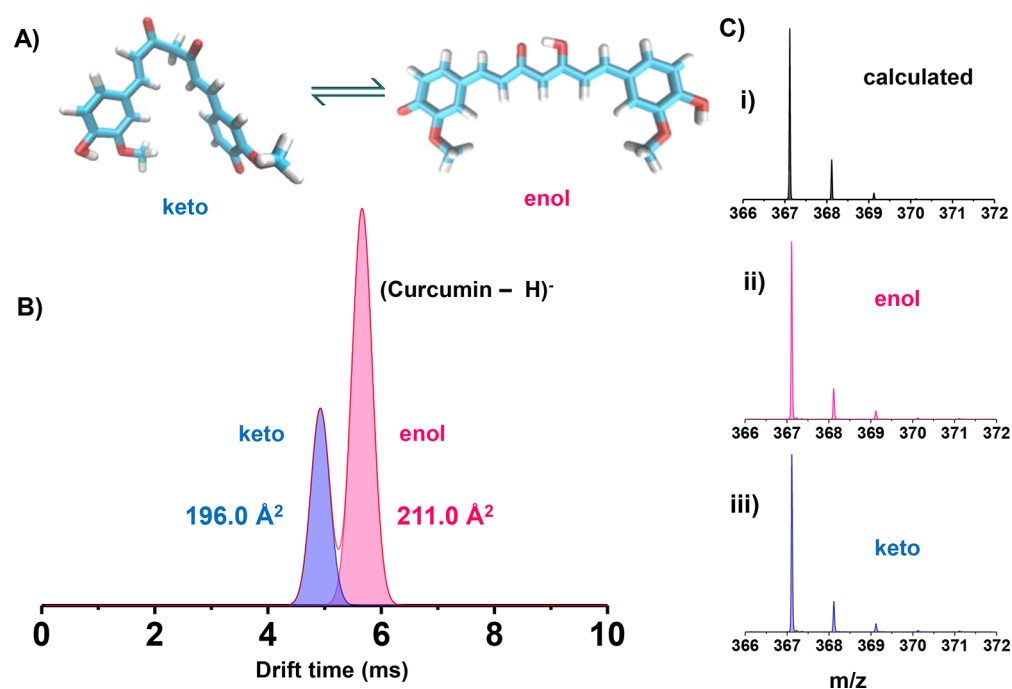


Figure 1. (A) Schematic representation of deprotonated keto–enol tautomers of curcumin. (B) Drift time profile of curcumin ($m/z = 367$) showing the two isomeric species with drift times of 4.92 and 5.72 ms, with CCS values, 196.0 and 211.0 Å², respectively. (C) Relative peak intensities of isotopologues of keto and enol tautomers of curcumin, which are matching with the calculated relative peak intensities of isotopologues.

experimentally and this represents a gap which we will address in this Article.

The bioavailability of curcumin is known to be enhanced by the presence of molecules such as piperine.^{26,27} An understanding of the preferential stabilization of the two forms by different molecules will help in formulating curcumin. There have been reports that curcumin gets transported across the blood–brain barrier (BBB).^{16,28–30} Its enhanced delivery into the brain is of importance to neurological diseases such as Alzheimer's.^{7,16,17,23,31–33}

A major problem in curcumin-based drugs is the low solubility of the molecule in an aqueous medium. An obvious choice to enhance solubility is cyclodextrins (CDs) and β -CD has been used extensively in medical formulations. However, the preferential stabilization of the keto–enol forms of curcumin is unclear from spectroscopy. Crystal structures of these supramolecular complexes are unknown.^{34–37}

A combination of ion mobility mass spectrometry, theoretical calculations including molecular docking and CCS calculations can reveal the structures of these complexes. In this Article, we propose the structures and conformations of the well-known enol and the far more elusive keto form of curcumin by using ion mobility mass spectrometry (IM MS). The CCS values measured from IM MS are compared with the calculated CCS values of the theoretically predicted isomers, confirming the structures. We identify the degree of bending of the keto tautomer using this method. We show that IM MS manifests the tautomers of curcumin and represents their solution phase populations, in this case. We show that the enol form of curcumin is selectively enhanced in the presence of piperine. The structures of keto \cap CD and enol \cap CD (the \cap symbol refers to partial encapsulation, A encapsulated in B is denoted as A \cap B).³⁸ are elucidated by using IM MS. The

experimental observations are fully supported by DFT, CCS, and molecular docking studies.

EXPERIMENTAL SECTION

Instrumentation. Mass Spectral Measurements. All mass spectrometric measurements were conducted using a Waters Synapt G2Si High Definition Mass Spectrometer equipped with electrospray ionization (ESI) and ion mobility (IM) separation techniques. All the samples were analyzed in negative ESI mode. More details about the measurements are given in Supporting Information (SI).

RESULTS AND DISCUSSION

Separation of Keto–Enol Forms of Curcumin by IM MS. Curcumin is a β -diketone system, which shows tautomerism between keto and enol forms. However, because of rapid interconvertibility of the tautomers, separation and complete characterization of the individual keto and enol forms remain challenging. Ion mobility mass spectrometry (IM MS) has power to separate ions not only by m/z ratio but also by their shape.^{39–45} It has the capability to separate isomers depending on the difference in their collision cross sections while passing through a buffer gas (as for example N₂ and He) in the mobility cell under the influence of a weak electric field. Curcumin solution (0.05 mM in methanol) was directly electrosprayed for the IM MS measurement. In the negative ion mode, the peak corresponding to $[M-H]^-$ (deprotonated form) was detected at m/z 367 along with its isotopologues 368 and 369. The molecule was ionized by losing a proton from the phenolic –OH. IM MS experiments were performed on the deprotonated form $[M-H]^-$. Two well-separated peaks were observed at 5.72 and 4.92 ms, as shown in Figure 1B. The highest intense peak came at 5.72 ms, whereas the weaker one arrived at 4.92 ms in the drift scale bar (Figure 1B). Two peaks

in the mobilogram represent the tautomeric nature of ionized curcumin. The corresponding species have the same chemical formula because the relative intensities of all the isotopologues are the same (see Figure 1C). The corresponding collision cross sections (CCSs) were 196.0 and 211.0 Å², respectively (Figure 1B).

CID of Keto–Enol Forms of Curcumin in the Transfer Cell. To get more insight into the structure of the isomers, collision-induced dissociation (CID) was performed. The spectrometer has two collision cells; trap CID (situated before IMS) and transfer CID (located after IMS). Transfer CID was used to carry out fragmentation after ion mobility separation.⁴⁶ This enables us to fragment both the tautomers individually. The *m/z* values, 149, 175, 191, and 217 were the fragmented species from the 4.92 ms tautomer (Figure S1A). The peaks at *m/z* 175 and 191 were specific to the keto form of curcumin.^{47,48} The 5.72 ms tautomer fragmented and gave peaks at *m/z* 134, 149, 173, and 217 (Figure S1B).^{47,48} The characteristic fragment of enol appeared at *m/z* 173.

Intensity ratio of the peaks gave an equilibrium constant of 4.5 for the enol–keto equilibrium (Figure S6), which is comparable with the solution phase.⁴⁹ Deprotonation from both the forms did not affect the equilibrium constant. More details are discussed later.

DFT and CCS Calculations of Different Structures of Curcumin. We generated four curcumin conformers (two for enol and two for keto) from our conformer searches and subsequent DFT optimization. The two enol conformers abbreviated as (CE1–H)[–] and (CE2–H)[–] and are shown in Figure 2A and B. We also generated two keto conformers

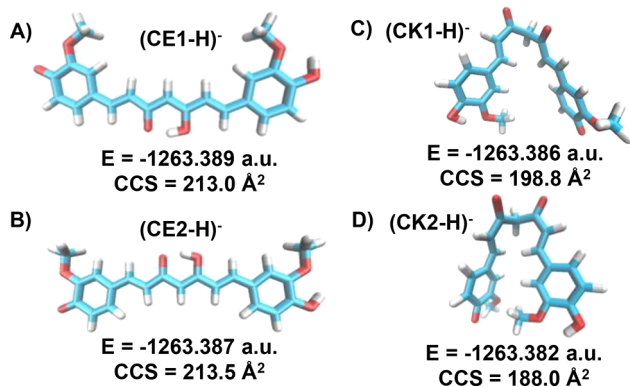


Figure 2. DFT optimized structures of deprotonated keto and enol tautomers of curcumin with their total energies and theoretically calculated CCS values. Here, CE and CK represent *cis*-enol and -keto, respectively. Panels A and B show different types of enol tautomers like (CE1–H)[–] and (CE2–H)[–], respectively, with optimized energies and CCS values. Panels C and D indicate the different types of keto tautomers like (CK1–H)[–] and (CK2–H)[–], respectively, with optimized energies and CCS values.

labeled (CK1–H)[–] and (CK2–H)[–], which are shown in Figures 2C and D. The letters C in the conformer names indicates the *cis* configurations about the –C–(C=O)–C–(C=O)–C– bonds, followed by E or K to indicate enol or keto. The more details on the naming of keto–enol tautomers are given in Figure S2. The numbers 1 or 2 indicate the energy rank for the same type of *cis* configurations so that (CE1–H)[–] was the lowest energy *cis*-enol tautomer and (CK1–H)[–] was the lowest energy *cis*-keto tautomer. Among the enol conformers, the energetic ordering was (CE1–H)[–] < (CE2–

H)[–] (+0.002 a.u.), where the energy relative to the (CE1–H)[–] is given in brackets. (CE1–H)[–] was the most stable tautomer and the energy difference between (CE1–H)[–] and (CE2–H)[–] is very small (0.002 a.u.) as they were quite similar in structure apart from the spatial position of the –OMe group, which was *cis* with respect to the keto–enolic group in the case of (CE1–H)[–] and *trans* in the case of (CE2–H)[–].

All of the enol tautomers were planar while the two keto structures were bent about the diketone group in varying degrees. It is convenient to introduce a bending angle to characterize the degree of this bending, rather than specify all the relevant dihedral angles in the seven-carbon chain bridging the two phenyl groups. The degree of bending of the seven carbon chain about its central carbon atom in the diketone group may be defined as the angle ACB, where C central carbon atom and A and B are the two carbon atoms located in the benzene rings which bond to the end atoms of the seven carbon chain, as shown in Figure S4. The bending angles of the (CK1–H)[–] and (CK2–H)[–] conformers were 75° and 65°, respectively. The relative stability of the keto conformers was indicated by their energetic ordering, (CK1–H)[–] < (CK2–H)[–] (+0.004 a.u.), where the difference between the conformer energy and (CK1–H)[–] energy is given in brackets. The L- and U-shaped conformations for the keto, (CK1–H)[–] and (CK2–H)[–], respectively (Figures 2C and D) were stabilized by weak intramolecular interactions, such as π – π interactions and van der Waals interactions between atoms in the seven-carbon chain and between the two benzene rings and their –O and –OMe functional groups, all of which contribute to lowering of the total energy. Because of these interactions, (CK2–H)[–] was more bent compared to both (CK1–H)[–].

The experimental difference in drift time reflected the planar enol and the L-shaped bent keto structures. The latter is more compact and it has a shorter drift time. The calculated CCSs of 213.0 Å² for (CE1–H)[–] and 198.8 Å² for (CK1–H)[–] matched well with our experimental result of 211.0 and 196.0 Å², for enol and keto, respectively (Table S1), which confirms that the enol form had a planar structure, and keto form has a bent structure with a bending angle of 75°. Hence, using this combined structural and energetic study along with a comparison of the CCS values with the experiment, we have confirmed the well-known structure of enol, and the likely candidate of the keto tautomer, including its degree of bending. We note that (CE1–H)[–] and (CE2–H)[–] were close in energy and have similar CCS values. Therefore, it is likely that they both are coexisting. However, for the keto form, though all the structures are similar in energy (shown in Table S1), their CCS values are widely different and therefore it is likely that only (CK1–H)[–] exists. The energy differences are in fact insignificant when the computational errors and the effective temperature of the ion mobility cell are considered.

Correlation between Solution- and Gas-Phase Structures of Curcumin. In solution, the enol form is stabilized by intramolecular H-bonding, while the keto form is stabilized by intermolecular H-bonding with the solvent.⁴⁹ In nonpolar solvents, populations of the enol form will be more compared to keto form. Reverse is the true for polar solvents.⁴⁹ In our IM MS study also same thing has happened. With change of solvent, from nonpolar to polar, the intensity of both the peaks changed drastically (Figure S5). With the increase of polarity of the solvent (from hexane to 1:1 methanol–water mixture), the intensity of the keto form was enhanced compared to the enol form. In a protic solvent, the keto form is enhanced

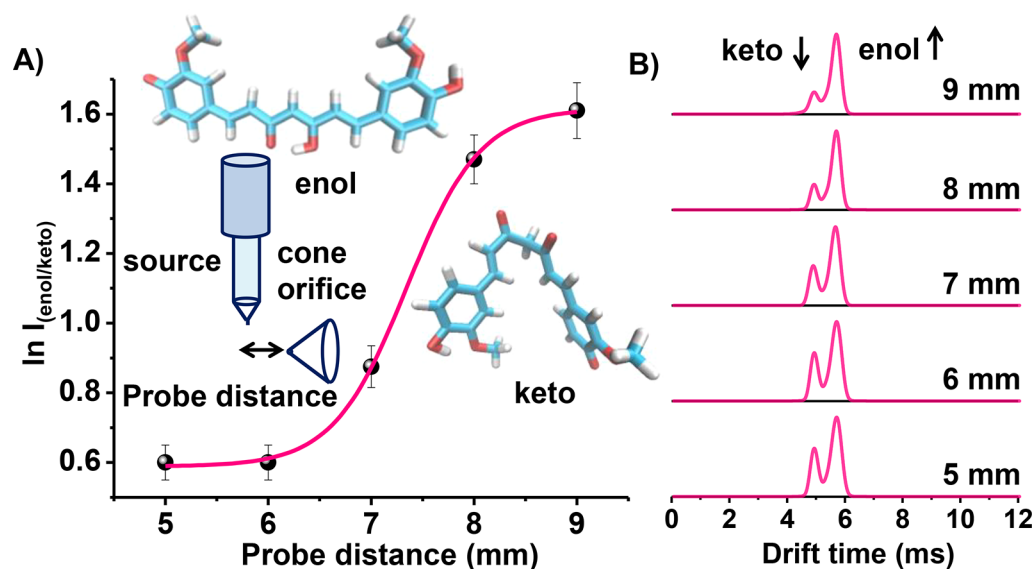


Figure 3. (A) Plot of the natural logarithm of keto/enol peak intensity ratios against different probe distances from 5 to 9 mm. (B) With the increase in probe distance, enol form enhances in intensity. The two structures are shown in panel A. A schematic representation of the probe distance parameter is illustrated in panel A.

because intermolecular hydrogen bonding with the solvent will be preferred compared to the intramolecular H-bonding. From the data presented in Figure S5, it is clear that the solution phase population is reflected in the gas phase, in this case. Condition of the ESI source of the instrument has great influence on the abundance of tautomers.^{50,51} To establish the solution and gas phase correlation and to support the structural information, three source parameters were varied while a few others were kept constant.^{50,52} Results are presented as follows: (1) The Synapt G2Si has a probe adjuster, through which the distance of the spraying position of the capillary to the cone orifice can be varied from 5 to 9 mm (Figure 3A). The ratio of the two tautomeric forms displays dramatic change in intensity with the variation of probe distance. In a very recent report, Xia et al. has shown that changing the probe position, desolvation temperature, capillary voltage, sample infusion flow rate and cone voltage, the relative populations of the tautomers can be changed in the case of *p*-hydroxybenzoic acid.⁵⁰ When the probe tip is close to the cone aperture, that is, under high field conditions, ions can preserve their solution based ionic structures. But when the distance between the spray needle and the entrance orifice is more, that is, under low field condition, gas phase ion population is enhanced. This phenomenon can be justified by charge ion evaporation and charge residue models. In our IM MS study, when the sprayer capillary was kept away from the cone orifice, the enol form was enhanced and the keto form was drastically reduced (Figure 3B). Therefore, with the increase in probe distance, the enol form got enhanced, which is more stable in the gas phase. As the probe distance is increased, the ions are going more into the gas phase as solvent evaporation is facilitated. But the drift time of both the tautomers, that is, their CCS values remains constant with the change of probe distance, which suggests that the structures of the two forms remain the same as in the solution state in this case.

(2) Temperature of the atmospheric pressure ion source also impacts the relative ratio of the tautomer populations. In our mass spectrometer, the temperature of the enclosed spray chamber is influenced mainly by the desolvation-gas temper-

ature (DT). To measure the effect of temperature on both the tautomeric forms, DT was varied from 40 to 600 °C (Figure S6A). With the increase of DT, the intensity of the keto form was enhanced (Figure S6B). Disruption of the enolic hydrogen bond with increase of temperature favored the shifting of the equilibrium toward the keto form. The same phenomenon has happened in solution phase.⁴⁹ The drift time values of the keto and enol forms did not change with the increase of temperature, which suggests that the same structures are retained in the gas phase, which are also the solution phase structures. The ratio of enol/keto forms was 4.5 (equilibrium constant) at a desolvation temperature of 40 °C and probe distance of 6 mm, which is comparable with the solution phase data from previous literature.⁴⁹

(3) We observed that the cone voltage had a great influence on the tautomeric ratio (Figure S7). As the cone voltage was raised, gaseous ions experienced acceleration in this region, collided with the background gases and underwent fragmentation.^{53–55} When the cone voltage was high, the keto form was favored and the reverse was true when the cone voltage was low. This can be because of the breakage of enolic hydrogen bond, and hence the conversions into the keto form. We have also performed the cone voltage study to see the different rates of insource fragmentation for the two tautomers. But, no additional change in fragmentation was seen with the increase of cone voltage. This is shown in Figure S8. This study supports the breakage of hydrogen bond with the increase of cone voltage, which results in conversion of enol to keto form.

In summary, variation of source parameters supported the correlation between gas phase and solution phase structures in this case. However, we are aware of the issues involved in the generalization of such studies. Therefore, we have limited the discussions of ESI MS data being reflective of solution phase structures to the present studies.

Comparison with the Solution Phase. Further, to confirm the solution phase tautomerism, we separated the keto–enol forms by ultraperformance liquid chromatography (UPLC) (Figure 4A). After the two tautomers were separated using UPLC, fragmentation (CID) of both the tautomeric

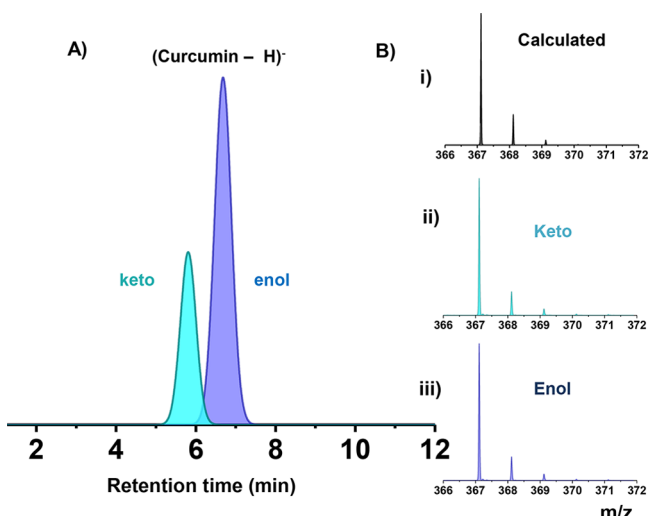


Figure 4. (A) UPLC separated keto enol tautomers of curcumin. (B) Relative peak intensities of isotopologues of keto and enol tautomers of curcumin, which are matching with the calculated peak intensities of isotopologues.

species was performed (Figure S9B). Here, the fragmentation pattern of each tautomer was matched with the CID data of ESI IM MS. This study further reinforced that the solution phase tautomeric structure of curcumin is retained in the gas phase in this case.

Interaction of Curcumin with Piperine. Piperine is a naturally occurring heterocyclic compound found in all forms of pepper (black, white, and green), and this molecule is responsible for its pungency and heat. Dietary polyphenols like piperine and curcumin have been studied for their effect on prevention of breast cancer.^{56,57} Mammosphere formation⁵⁸ is a marker of breast cancer cell lines. Curcumin and black pepper compounds both inhibited mammosphere formation. They did not also cause any toxicity, therefore showing that

curcumin, piperine, or piperine–curcumin adduct could be possible cancer preventive agents. On the other hand, piperine enhances the bioavailability of curcumin. However, it is still not clearly understood that which tautomeric form of curcumin is better stabilized by it. Ion mobility mass spectrometry showed that with the increase of the concentration of piperine, the intensity of the enol form was enhanced and the population of keto form was decreased (Figure 5A). This shows that with the use of piperine, one can selectively enhance the enol form. The supramolecular adduct of curcumin–piperine was detected in ESI MS (Figure S10). The preferential stabilization of the enol form in the adduct and its enhanced population in solution in the presence of piperine was reflected in the IM MS measurement. To understand the mechanism of the enhancement of the enol form, a DFT study was performed. We took four lowest energy tautomers: 2 enols [(CE1–H)[−] and (CE2–H)[−]] and 2 ketos [(CK1–H)[−] and (CK2–H)[−]]. Each tautomer was interacted with piperine considering the different possibilities of hydrogen bonds and π – π interactions. The optimized geometries are shown in Figures S11–S15 and the calculated relative energies are listed in Table S2. Among the lowest energy structures of the complexes of each tautomer of curcumin with piperine (Table S4), the difference in the energies of the complexes with (CE1–H)[−] (−23.51 kcal/mol) and (CE2–H)[−] (−20.60 kcal/mol) is marginal as the complexes are stabilized through similar π – π stacking interaction. The complex of (CK1–H)[−] with piperine is stabilized by both hydrogen bonding and π – π stacking interactions between six-membered rings of piperine and aliphatic double bond of curcumin. These interactions are absent in the case of (CK2–H)[−]. Because of this, the interaction energy is more negative for (CK1–H)[−] (−23.08 kcal/mol) than for (CK2–H)[−] (−22.18 kcal/mol) (Table S4). However, the complexes of piperine with enol form of curcumin are more stable than that of the keto form, with respect to the total energy.

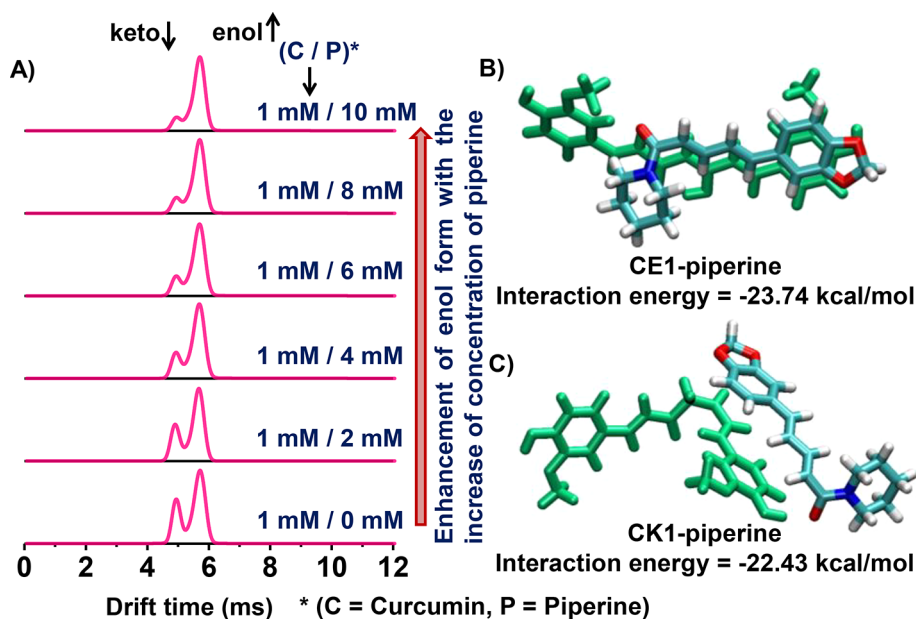


Figure 5. (A) Shift of the keto–enol equilibrium toward the enol form with increase in piperine concentration in the solution. (B and C) DFT optimized lowest energy structures of CE1–piperine and CK1–piperine complexes, respectively. Green color is used for keto and enol tautomers of curcumin.

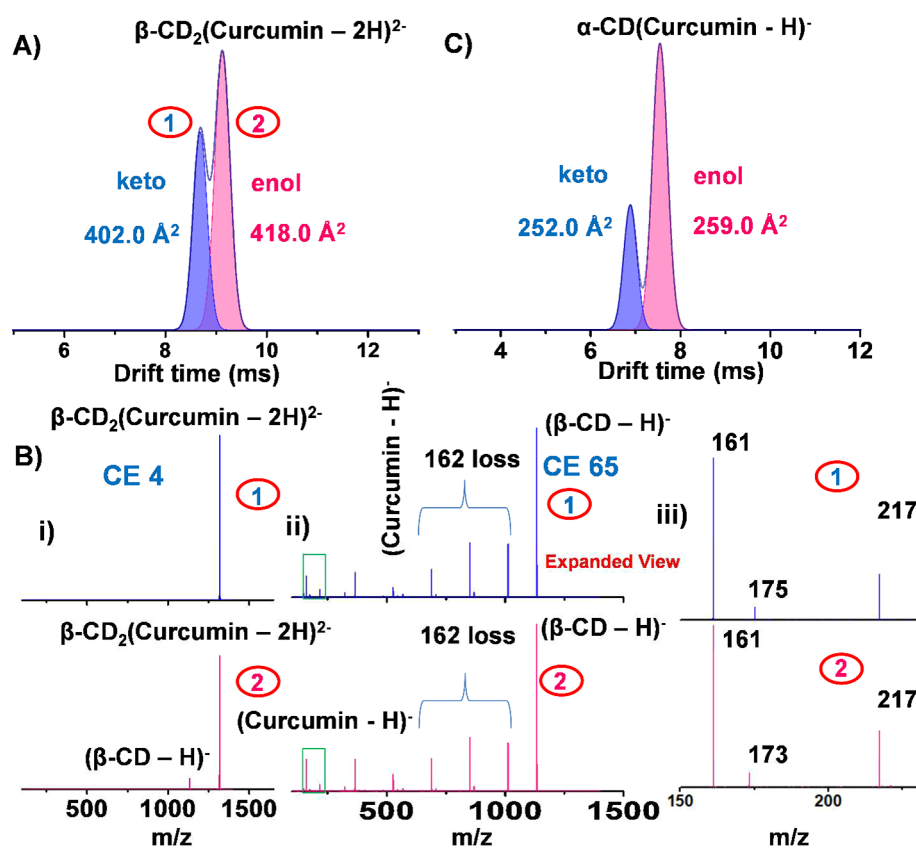


Figure 6. (A) Drift time profile of curcumin- β -cyclodextrin (1:2) inclusion complex; two peaks are indicating the isomeric structures. (B) (i and ii) MSMS fragmentation at transfer CID cell of both the isomeric peaks 1 and 2 shown in panel A, with different collision energies, 4 and 65 V, respectively. (iii) Expanded view of the m/z region 150–230, shown in panel ii as a box. (C) Two isomeric species of the α -cyclodextrin-curcumin (1:1) complex.

The large difference in the energies of the enol ($E_{(\text{CE1-H})^-} = -1263.389$ au) and keto ($E_{(\text{CK1-H})^-} = -1263.386$ au) forms of curcumin is also preserved during their complexation with piperine. Further, similar trend was observed for the proton added forms of the respective species (see Table S3). The interaction energy of CE1 is marginally higher than CK1 (Figure 5B and C).

Determination of Structures of Curcumin \cap Cyclodextrin Complexes. Cyclodextrins (CDs) are cyclic oligosaccharides with a lipophilic central cavity and hydrophilic outer surface. Hydrophilic drug/CD complexes are synthesized by the inclusion of lipophilic drug moieties in the central CD cavity. While the guest molecule is safeguarded by the lipophilic cavity from the aqueous environment, the polar outer surface of the CD molecule furnishes the solubilizing effect. CDs have been used frequently as solubilizing, stabilizing, and drug delivery agents in pharmaceutical preparations for enhancing the bioavailability of the drug.⁵⁹ We predicted the structures of the isomers of curcumin \cap CD complexes using molecular docking and then applied the projection approximation (PA) method⁶⁰ to compute their CCS values and compared them with the experimental values obtained from IMS MS to confirm the structures.

A mixture of curcumin and β -CD was infused through a standard electrospray ion source into the spectrometer at a concentration of ~ 0.05 mM (water/methanol, 1:1). The negative ion peak at m/z 1317 (2:1 β -CD:curcumin inclusion complex) was selected and passed through the ion mobility cell. Two distinct isomeric peaks were detected with the drift

time values of 8.69 and 9.13 ms, respectively (Figure 6A). The CCS values of the two peaks were 402.0 and 418.0 \AA^2 , respectively. To get more information about the structure, CID fragmentation was performed in the transfer cell. We selectively fragmented both the isomers. At a collision energy 4 V, β -CD loss was observed from the 9.13 ms drift time isomer, while the other isomer with drift time of 8.69 ms did not fragment at that energy. This suggested that the latter isomer is slightly more stable compared to the former. Further increase of collision energy gave rise to the curcumin molecular ion peak and the sequential loss of 162 from CD (Figure 6B(ii)). This loss is due to the glucopyranose unit, typical signature of the CD.⁶¹ Upon expanding the mass range of m/z 150–230 for both the isomers, we find that the peaks at m/z 173 and 175 are, respectively the fragmented species from the isomers at drift times of 9.13 and 8.69 ms (Figure 6B(iii)). This confirmed that the isomers were derived from the enol and keto tautomers of curcumin, respectively. We expanded our study to the α -CD-curcumin complex. In this case, the 1:1 inclusion complex (α -CD:curcumin) was chosen and transferred through the ion mobility cell. Here also, two isomeric peaks were detected. The corresponding CCS and drift time values were 252.0 and 259.0 \AA^2 and 6.89 and 7.55 ms, respectively (Figure 6C). The CCS values of the curcumin \cap CD complexes provide additional verification of the bent structure of keto as a planar keto form will show identical CCS value as that of the enol.

Molecular Docking Study of Curcumin \cap Cyclodextrin Complexes. Molecular docking simulations of curcumin

tautomers, CE1 and CK1 with α - and β -CD monomers and β -CD dimers were used to determine the structures of their inclusion complexes, using the Autodock 4.2 and AutoDock Tools programs. The interactions are basically vdW, hydrogen bonding, electrostatic, and hydrophobic in nature, and therefore, a force field with these terms as implemented in the Autodock program was appropriate. As our primary objective was to determine the structures of the complexes by comparing their calculated CCS values with the experiment, we did not perform any DFT calculations.^{62–65} This is reasonable since the majority of the interactions are non-covalent. The docking search was designed to perform global optimization (GO) for the two-molecule problem with a single curcumin (lowest energy enol CE1 and keto CK1) as the “ligand” and α -CD as the “receptor”. We obtained ten lowest energy isomers for CE1/ α -CD complex with the CE1 stabilized inside the cavity of CD. The structures were identical with slight changes in the orientation of CE1 and showed similar binding energies (BEs) in the range of -6.55 to -6.46 kcal/mol. Docking studies on CK1/ α -CD complex also gave ten lowest energy structures with the BEs in the range of -6.32 to -6.30 kcal/mol. The CCS values of the structures with lowest BE for CE1/ α -CD (246.0 \AA^2) and for CK1/ α -CD (243.0 \AA^2) matched closely with the experimental data (Figure 6C) as shown in the Figures 7A and B. The Autodock 4.2

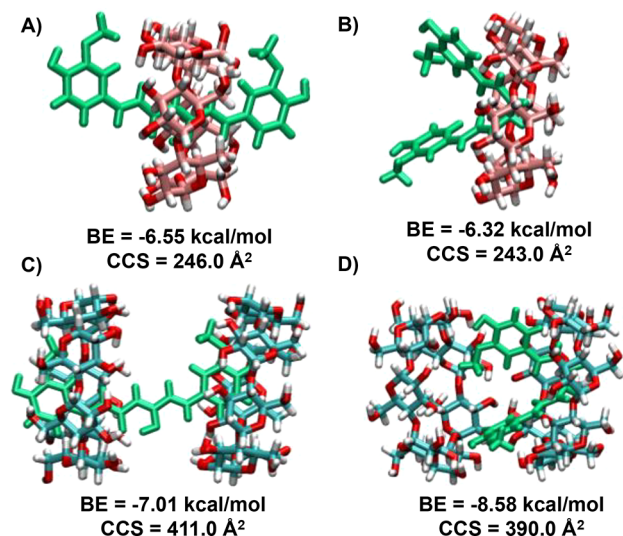


Figure 7. (A and B) CE1 and CK1 docked α -cyclodextrin, respectively. (C and D) Same for β -cyclodextrin dimer. The binding energies and CCS values are listed below the structure. The structures shown are the energy minimum forms.

program cannot simultaneously carry out the GO problem for three molecules. Hence for the case of 2:1 β -CD:curcumin complexes, we followed different procedures to obtain an approximate solution to the three molecules GO problem:

(1) We first docked the curcumin tautomer (CE1 and CK1 separately as the “ligand”) with one β -CD as the “receptor” (Figure S18). Then, taking its newly docked lowest energy structure (Figure S18) as the “receptor”, we subsequently docked the second β -CD as the “ligand” (Figure S19).

(2) In another approach, various initial configurations of the two β -CD molecules were considered by arranging them in HH configuration (H stands for head, see molecular docking in SI), with different separations [4 (Figure S20B), 5 (Figure

7C), and 6 \AA (Figure S20A) for CE1/ β -CD] and angles [$\theta = 30^\circ$ (Figure S21A), 40° (Figure 7D), and 65° (Figure S21B) for CK1/ β -CD] between their central axis of rotation. Now, this double CD system was treated as the “receptor” molecule and the curcumin molecule (CE1 and CK1 separately) as the “ligand”. Additional details are included in SI. The lowest energy structures of the complexes were obtained from the second approach for the three molecule GO problem. The structures of CE1/ β -CD resembled a dumbbell with a separation of 5 \AA between the two CDs, with a BE of -7.03 kcal/mol and with the calculated CCS value of 411.0 \AA^2 (Figure 7C). In the lowest energy structure of CK1/ β -CD, one end of the L-shaped keto form (CK1) was encapsulated between the two CDs lying at an angle of 40° and the other end of the keto was protruding outward from the gap. This structure showed a BE of -8.58 kcal/mol and calculated CCS value of 390.0 \AA^2 (Figure 7D). The calculated CCS values of the lowest energy structures were in close agreement with the experimental CCS values (Tables S5 and S6), which supported the proposed structures of the inclusion complexes.

CONCLUSION

Our study shows that the two structural forms of curcumin, namely, keto and enol forms can be isolated in the gas phase. The gas phase populations represent the solution phase populations in this case. We found a new bent keto structure by ion mobility studies and verified its structure including its degree of bending, by simulations. The enol form can be selectively stabilized by the presence of piperine. Both the forms can be complexed with cyclodextrin, although there is a slight preference for the keto form for the β -CD dimer. The IM MS experiments and theoretical calculations that were performed by docking studies have enabled us to obtain exhaustive structural information about the curcumin and curcumin/ β -CD complexes which could not be unambiguously characterized through standard methods such as X-ray crystallography and NMR. We could predict the actual structure of curcumin/ β -CD inclusion complexes with the help of IM MS measurements and theoretical CCS calculations. This study shows the application of IM MS to identify the structural details of commonly used natural products. Insights from the studies such as the stabilization of enol by piperine will be of immediate value to the medical community as the enol form is active toward the Alzheimer’s disease.

ASSOCIATED CONTENT

Supporting Information

The Supporting Information is available free of charge on the ACS Publications website at DOI: 10.1021/acs.analchem.7b05231.

Experimental details, computational details, DFT optimized structures of curcumin, curcumin–piperine complexes, solvent dependent study, and cone voltage dependent study (PDF)

Molecular docking study and CCS calculations (PDF)

AUTHOR INFORMATION

Corresponding Author

*Fax: +91-44 2257-0545. E-mail: pradeep@iitm.ac.in.

ORCID

Venkatesan Subramanian: 0000-0003-2463-545X

Thalappil Pradeep: 0000-0003-3174-534X

Notes

The authors declare no competing financial interest.

ACKNOWLEDGMENTS

We thank the Department of Science and Technology, Government of India, for constantly supporting our research program on nanomaterials. A.N. thanks IIT Madras for a doctoral fellowship. P.C. thanks the Council of Scientific and Industrial Research (CSIR) for her research fellowship. A.B. thanks IIT Madras for a Postdoctoral fellowship. S.K.M. thanks DST-INSPIRE for his senior research fellowship.

REFERENCES

- (1) Nelson, K. M.; Dahlin, J. L.; Bisson, J.; Graham, J.; Pauli, G. F.; Walters, M. A. *J. Med. Chem.* **2017**, *60*, 1620–1637.
- (2) Payton, F.; Sandusky, P.; Alworth, W. L. *J. Nat. Prod.* **2007**, *70*, 143–146.
- (3) Sanphui, P.; Goud, N. R.; Khandavilli, U. B. R.; Bhanoth, S.; Nangia, A. *Chem. Commun.* **2011**, *47*, 5013–5015.
- (4) Su, H.; He, H.; Tian, Y.; Zhao, N.; Sun, F.; Zhang, X.; Jiang, Q.; Zhu, G. *Inorg. Chem. Commun.* **2015**, *55*, 92–95.
- (5) Argyropoulou, A.; Aligiannis, N.; Trougakos, I. P.; Skaltsounis, A.-L. *Nat. Prod. Rep.* **2013**, *30*, 1412–1437.
- (6) Barry, J.; Fritz, M.; Brender, J. R.; Smith, P. E. S.; Lee, D.-K.; Ramamoorthy, A. *J. Am. Chem. Soc.* **2009**, *131*, 4490–4498.
- (7) Wanninger, S.; Lorenz, V.; Subhan, A.; Edelmann, F. T. *Chem. Soc. Rev.* **2015**, *44*, 4986–5002.
- (8) Mitra, K.; Gautam, S.; Kondaiah, P.; Chakravarty, A. R. *Angew. Chem., Int. Ed.* **2015**, *54*, 13989–13993.
- (9) Renfrew, A. K.; Bryce, N. S.; Hambley, T. W. *Chem. Sci.* **2013**, *4*, 3731–3739.
- (10) Jovanovic, S. V.; Boone, C. W.; Steenken, S.; Trinoga, M.; Kaskey, R. B. *J. Am. Chem. Soc.* **2001**, *123*, 3064–3068.
- (11) Jovanovic, S. V.; Steenken, S.; Boone, C. W.; Simic, M. G. *J. Am. Chem. Soc.* **1999**, *121*, 9677–9681.
- (12) Vemula, P. K.; Li, J.; John, G. *J. Am. Chem. Soc.* **2006**, *128*, 8932–8938.
- (13) Pu, H.-L.; Chiang, W.-L.; Maiti, B.; Liao, Z.-X.; Ho, Y.-C.; Shim, M. S.; Chuang, E.-Y.; Xia, Y.; Sung, H.-W. *ACS Nano* **2014**, *8*, 1213–1221.
- (14) Jordan, W. C.; Drew, C. R. *J. Natl. Med. Assoc.* **1996**, *88*, 333–333.
- (15) Ran, C.; Xu, X.; Raymond, S. B.; Ferrara, B. J.; Neal, K.; Bacskai, B. J.; Medarova, Z.; Moore, A. *J. Am. Chem. Soc.* **2009**, *131*, 15257–15261.
- (16) Tiwari, S. K.; Agarwal, S.; Seth, B.; Yadav, A.; Nair, S.; Bhatnagar, P.; Karmakar, M.; Kumari, M.; Chauhan, L. K. S.; Patel, D. K.; Srivastava, V.; Singh, D.; Gupta, S. K.; Tripathi, A.; Chaturvedi, R. K.; Gupta, K. C. *ACS Nano* **2014**, *8*, 76–103.
- (17) Zhang, X.; Tian, Y.; Li, Z.; Tian, X.; Sun, H.; Liu, H.; Moore, A.; Ran, C. *J. Am. Chem. Soc.* **2013**, *135*, 16397–16409.
- (18) Zhang, J.; Liang, Y.-C.; Lin, X.; Zhu, X.; Yan, L.; Li, S.; Yang, X.; Zhu, G.; Rogach, A. L.; Yu, P. K. N.; Shi, P.; Tu, L.-C.; Chang, C.-C.; Zhang, X.; Chen, X.; Zhang, W.; Lee, C.-S. *ACS Nano* **2015**, *9*, 9741–9756.
- (19) Banerjee, S.; Chakravarty, A. R. *Acc. Chem. Res.* **2015**, *48*, 2075–2083.
- (20) Girish, C.; Pradhan, S. C. *J. Pharmacol. Pharmacother.* **2012**, *3* (2), 149–155.
- (21) Aggarwal, B. B.; Harikumar, K. B. *Int. J. Biochem. Cell Biol.* **2009**, *41*, 40–59.
- (22) Hassaninasab, A.; Hashimoto, Y.; Tomita-Yokotani, K.; Kobayashi, M. *Proc. Natl. Acad. Sci. U. S. A.* **2011**, *108*, 6615–6620.
- (23) Yanagisawa, D.; Shirai, N.; Amatsubo, T.; Taguchi, H.; Hirao, K.; Urushitani, M.; Morikawa, S.; Inubushi, T.; Kato, M.; Kato, F.; Morino, K.; Kimura, H.; Nakano, I.; Yoshida, C.; Okada, T.; Sano, M.;

Wada, Y.; Wada, K.-n.; Yamamoto, A.; Tooyama, I. *Biomaterials* **2010**, *31*, 4179–4185.

(24) Kolev, T. M.; Velcheva, E. A.; Stamboliyska, B. A.; Spitteller, M. *Int. J. Quantum Chem.* **2005**, *102*, 1069–1079.

(25) Galasso, V.; Kovač, B.; Modelli, A.; Ottaviani, M. F.; Pichierri, F. *J. Phys. Chem. A* **2008**, *112*, 2331–2338.

(26) Prasad, S.; Tyagi, A. K.; Aggarwal, B. B. *Cancer Res. Treat* **2014**, *46*, 2–18.

(27) Shoba, G.; Joy, D.; Joseph, T.; Majeed, M.; Rajendran, R.; Srinivas, P. S. S. R. *Planta Med.* **1998**, *64*, 353–356.

(28) Pahuja, R.; Seth, K.; Shukla, A.; Shukla, R. K.; Bhatnagar, P.; Chauhan, L. K. S.; Saxena, P. N.; Arun, J.; Chaudhari, B. P.; Patel, D. K.; Singh, S. P.; Shukla, R.; Khanna, V. K.; Kumar, P.; Chaturvedi, R. K.; Gupta, K. C. *ACS Nano* **2015**, *9*, 4850–4871.

(29) Krol, S.; Macrez, R.; Docagne, F.; Defier, G.; Laurent, S.; Rahman, M.; Hajipour, M. J.; Kehoe, P. G.; Mahmoudi, M. *Chem. Rev.* **2013**, *113*, 1877–1903.

(30) Cui, Y.; Zhang, M.; Zeng, F.; Jin, H.; Xu, Q.; Huang, Y. *ACS Appl. Mater. Interfaces* **2016**, *8*, 32159–32169.

(31) Randino, R.; Grimaldi, M.; Persico, M.; De Santis, A.; Cini, E.; Cabri, W.; Riva, A.; D'Errico, G.; Fattorusso, C.; D'Ursi, A. M.; Rodriguez, M. *Sci. Rep.* **2016**, *6*, 38846.

(32) Lim, G. P.; Chu, T.; Yang, F.; Beech, W.; Frautschy, S. A.; Cole, G. M. *J. Neurosci.* **2001**, *21*, 8370–8377.

(33) Chojnacki, J. E.; Liu, K.; Yan, X.; Toldo, S.; Selden, T.; Estrada, M.; Rodriguez-Franco, M. I.; Halquist, M. S.; Ye, D.; Zhang, S. *ACS Chem. Neurosci.* **2014**, *5*, 690–699.

(34) Heo, D. N.; Ko, W.-K.; Moon, H.-J.; Kim, H.-J.; Lee, S. J.; Lee, J. B.; Bae, M. S.; Yi, J.-K.; Hwang, Y.-S.; Bang, J. B.; Kim, E.-C.; Do, S. H.; Kwon, I. K. *ACS Nano* **2014**, *8*, 12049–12062.

(35) Yadav, V. R.; Suresh, S.; Devi, K.; Yadav, S. *AAPS PharmSciTech* **2009**, *10*, 752.

(36) Mangolim, C. S.; Moriwaki, C.; Nogueira, A. C.; Sato, F.; Baesso, M. L.; Neto, A. M.; Matioli, G. *Food Chem.* **2014**, *153*, 361–370.

(37) Yallapu, M. M.; Jaggi, M.; Chauhan, S. C. *Macromol. Biosci.* **2010**, *10*, 1141–1151.

(38) Lehn, J.-M. In *Supramolecular Chemistry*; Wiley-VCH Verlag GmbH & Co. KGaA: Weinheim, Germany, 2006; pp 1–9.

(39) Zhou, M.; Dagan, S.; Wysocki, V. H. *Angew. Chem., Int. Ed.* **2012**, *51*, 4336–4339.

(40) Weston, D. J.; Bateman, R.; Wilson, I. D.; Wood, T. R.; Creaser, C. S. *Anal. Chem.* **2005**, *77*, 7572–7580.

(41) Hofmann, J.; Hahm, H. S.; Seeberger, P. H.; Pagel, K. *Nature* **2015**, *526*, 241.

(42) Domalain, V.; Hubert-Roux, M.; Tognetti, V.; Joubert, L.; Lange, C. M.; Rouden, J.; Afonso, C. *Chem. Sci.* **2014**, *5*, 3234–3239.

(43) Hofmann, J.; Stuckmann, A.; Crispin, M.; Harvey, D. J.; Pagel, K.; Struwe, W. B. *Anal. Chem.* **2017**, *89*, 2318–2325.

(44) Gray, C. J.; Schindler, B.; Migas, L. G.; Pičmanová, M.; Allouche, A. R.; Green, A. P.; Mandal, S.; Motawia, M. S.; Sánchez-Pérez, R.; Bjarnholt, N.; Möller, B. L.; Rijs, A. M.; Barran, P. E.; Compagnon, I.; Evers, C. E.; Flitsch, S. L. *Anal. Chem.* **2017**, *89*, 4540–4549.

(45) Chakraborty, P.; Baksi, A.; Mudedla, S. K.; Nag, A.; Paramasivam, G.; Subramanian, V.; Pradeep, T. *Phys. Chem. Chem. Phys.* **2018**, *20*, 7593.

(46) Schröder, D.; Buděšinský, M.; Roithová, J. *J. Am. Chem. Soc.* **2012**, *134*, 15897–15905.

(47) Jiang, H.; Somogyi, Á.; Jacobsen, N. E.; Timmermann, B. N.; Gang, D. R. *Rapid Commun. Mass Spectrom.* **2006**, *20*, 1001–1012.

(48) Kawano, S.-i.; Inohana, Y.; Hashi, Y.; Lin, J.-M. *Chin. Chem. Lett.* **2013**, *24*, 685–687.

(49) Bhatia, N. K.; Kishor, S.; Katyal, N.; Gogoi, P.; Narang, P.; Deep, S. *RSC Adv.* **2016**, *6*, 103275–103288.

(50) Xia, H.; Attygalle, A. B. *Anal. Chem.* **2016**, *88*, 6035–6043.

(51) Anwar, A.; Psutka, J.; Walker, S. W. C.; Dieckmann, T.; Janizewski, J. S.; Larry Campbell, J.; Scott Hopkins, W. *Int. J. Mass Spectrom.* **2018**, *429*, 174.

- (52) Ghosh, D.; Baksi, A.; Mudedla, S. K.; Nag, A.; Ganayee, M. A.; Subramanian, V.; Pradeep, T. *J. Phys. Chem. C* **2017**, *121*, 13335–13344.
- (53) Pertel, R. *Int. J. Mass Spectrom. Ion Phys.* **1975**, *16*, 39–52.
- (54) Katta, V.; Chowdhury, S. K.; Chait, B. T. *Anal. Chem.* **1991**, *63*, 174–178.
- (55) Hunt, S. M.; Sheil, M. M.; Belov, M.; Derrick, P. J. *Anal. Chem.* **1998**, *70*, 1812–1822.
- (56) Zheng, J.; Zhou, Y.; Li, Y.; Xu, D.-P.; Li, S.; Li, H.-B. *Nutrients* **2016**, *8*, 495.
- (57) Park, W.; Amin, A. R. M. R.; Chen, Z. G.; Shin, D. M. *Cancer Prev. Res.* **2013**, *6*, 387–400.
- (58) Manuel Iglesias, J.; Beloqui, I.; Garcia-Garcia, F.; Leis, O.; Vazquez-Martin, A.; Eguiara, A.; Cufi, S.; Pavon, A.; Menendez, J. A.; Dopazo, J.; Martin, A. G. *PLoS One* **2013**, *8*, e77281.
- (59) Jana, B.; Mohapatra, S.; Mondal, P.; Barman, S.; Pradhan, K.; Saha, A.; Ghosh, S. *ACS Appl. Mater. Interfaces* **2016**, *8*, 13793–13803.
- (60) Siu, C.-K.; Guo, Y.; Saminathan, I. S.; Hopkinson, A. C.; Siu, K. W. M. *J. Phys. Chem. B* **2010**, *114*, 1204–1212.
- (61) Nag, A.; Baksi, A.; Krishnapriya, K. C.; Gupta, S. S.; Mondal, B.; Chakraborty, P.; Pradeep, T. *Eur. J. Inorg. Chem.* **2017**, *2017*, 3072–3079.
- (62) Muhammad, E. F.; Adnan, R.; Latif, M. A. M.; Abdul Rahman, M. B. *J. Inclusion Phenom. Macrocyclic Chem.* **2016**, *84*, 1–10.
- (63) Shityakov, S.; Salmas, R. E.; Durdagi, S.; Roewer, N.; Förster, C.; Broscheit, J. *J. Mol. Struct.* **2017**, *1134*, 91–98.
- (64) Zhao, Q.; Zhang, W.; Wang, R.; Wang, Y.; Ouyang, D. *Curr. Pharm. Des.* **2017**, *23* (3), 522–531.
- (65) Wang, R.; Zhou, H.; Siu, S. W. I.; Gan, Y.; Wang, Y.; Ouyang, D. *J. Nanomater.* **2015**, *2015*, 193049.